

Magnetic resonance, hyperthermia and oncology

Rama Jayasundar*[#], Laurance D. Hall[†] and Norman M. Bleehen*

*Clinical Oncology and Radiotherapeutics Unit, Medical Research Council, Hills Road, Cambridge CB2 2QH, UK

[†]Herchel Smith Laboratory for Medicinal Chemistry, Cambridge University School of Clinical Medicine, University Forvie Site, Robinson Way, Cambridge CB2 2PZ, UK

[#]Present address: Department of NMR, All India Institute of Medical Sciences, Ansari Nagar, New Delhi 110 029, India

Hyperthermic oncology deals with selective tumour cell killing by induced local or general heating to temperatures between 41°C and 45°C. The technique of magnetic resonance (MR) has been used for the non-invasive study of metabolic changes occurring as a result of hyperthermia, as well as for delivering hyperthermia using the radiofrequency coils used for the MR studies. This study demonstrates the feasibility of combining the fields of MR and hyperthermic oncology successfully and presents the results from unanesthetized tumour-bearing mice. The efficiencies of both heating and MR signal collection were maximized by the use of the same coil, tuned to the phosphorus resonance frequency at 2.0 T.

PHYSIOLOGICAL studies both under normal and pathological conditions have always been important to medical science. While studies under normal conditions are crucial for understanding the functioning of a system, those under pathological conditions are important for studying the mechanisms of disease in order to design appropriate treatments. A combination of techniques is usually used to maximize the information in the study and diagnosis of many pathologies. This paper discusses how such a combination can be used successfully in three major areas of research, namely, magnetic resonance (MR), oncology and hyperthermia. Since each area is vast, a comprehensive introduction to each is not possible. Introduction to the physical aspects of hyperthermia, relevant to this work, is covered in detail and that for the others kept to a minimum for brevity.

Many major technological advances have been applied in biological and clinical research: the resulting improvements in instrumentation have helped in conducting more accurate and elegant experiments to enable the living system to be interrogated. Many metabolic studies to date, however, have been invasive to varying degrees. This implies that the metabolism is often disrupted during the process of extraction of the sample and consequently, the results may not be representative of the *in vivo* situation. In the last three decades, however, a range of non-invasive biophysical techniques has been

developed, of which MR has proved to be the most versatile. In biological studies, MR imaging (MRI) is not a completely new technique since there are other imaging methods available. However, MR spectroscopy (MRS) is the only technique in clinical medicine that provides non-invasive access to living chemistry *in situ*.

With its increasing incidence, cancer has become a major problem in this century. Cancer is uncontrolled cell growth, uncoordinated with that of normal cells. The field of cancer research, i.e. oncology, can be divided into four major areas, namely causation, biology, diagnosis and therapy. The current therapeutic modalities for cancer are surgery, radiotherapy, chemotherapy and immunotherapy, with hyperthermia being an experimental/adjunct therapeutic modality^{1,2}.

Hyperthermia

The tumour cell kill by hyperthermia is accomplished by heating the tumour to temperatures between 41°C and 45°C, either by local or general heating¹. Although extensive *in vitro* studies have been carried out to investigate the associated biochemical changes resulting from hyperthermia, much *in vivo* work is required before extrapolating the *in vitro* results to clinical situations. The processes underlying thermal cell kill are not fully understood as yet and *in vivo* MRS is an ideal non-invasive technique for studying the effects of hyperthermia. Various techniques have been developed for producing hyperthermia for cancer therapy. These include the use of electromagnetic (EM) radiation in both the radiofrequency (RF) (1–100 MHz) and microwave (100 MHz – 2 GHz) ranges, ultrasound, isolated vascular perfusion, and wax baths^{1,2}. Of these EM, is the most widely used and is given a brief introduction because of its relevance to this work.

Interaction of EM waves with materials

The electric (*E*) and magnetic (*B*) fields are the two basic components associated with EM waves. The Maxwell's equations³ relate these fields to their sources and are shown below in both integral and differential forms.

*For correspondence: (e-mail: ramaj@medinst.ernet.in)

$$\int_s \epsilon_0 E \cdot ds = \int_v \rho_v dv \quad (\nabla \cdot \epsilon_0 E = \rho_v), \quad (1)$$

$$\int_s B \cdot ds = 0 \quad (\nabla \cdot B = 0), \quad (2)$$

$$\int_l E \cdot dl = -\frac{d}{dt} \int_s B \cdot ds \quad \left(\nabla \times E = -\frac{\partial B}{\partial t} \right), \quad (3)$$

$$\int_l \frac{B}{\mu_0} \cdot dl = \int_s J \cdot ds + \frac{d}{dt} \int_s E \cdot ds \quad \left(\nabla \times \frac{B}{\mu_0} = J + \frac{\partial \epsilon_0 E}{\partial t} \right). \quad (4)$$

In these equations μ_0 ($= 4\pi \times 10^{-7}$ Henry/m) and ϵ_0 ($= 8.854 \times 10^{-12}$ Faraday/m) are the permeability and permittivity of free space, respectively. J is the source current density and ρ_v is the volume charge density.

When an electric or magnetic field is impressed upon a material, it exerts forces on the constituent charged particles, resulting in their displacement or rearrangement. This modifies the impressed fields and results in a change in the properties of wave propagation. There are three basic mechanisms that can describe the interaction of EM waves with tissues. They are: (i) Displacement or drift of the conduction (free) electrons and ions in the tissue as a result of the force exerted by the EM fields. (ii) Polarization of atoms and molecules to produce dipole moments. (iii) Orientation of the existing dipoles in the direction of the applied electric field.

As a result of (i), there will be a conduction current, $I_c = \sigma E_m$, where E_m is the electric field inside the material and σ is the conductivity of the material. The other two mechanisms are related to the bound charges (not free) existing in the material. Polarization, for example, is related to displacement of the bound negative electron cloud from the equilibrium position relative to the positive nucleus (Figure 1 a). Orientational polarization occurs in materials possessing permanent electric dipoles, which are randomly oriented in the absence of an external field, but undergo an orientation towards the applied electric field vector by an amount depending on the strength of E . Water is a common example of a substance exhibiting this effect (Figure 1 b).

As a result of these polarization effects, there will be an additional polarization charge inside the material as well as polarization currents resulting from the displacement of the charges in the time-varying field. These generated charges and currents are new sources for electric and magnetic fields and Maxwell's equations should be modified accordingly. For example, eq. (1) (Gauss's law for the electric field) is modified to

$$\nabla \cdot \epsilon_0 E = \rho_v + \rho_p, \quad (5)$$

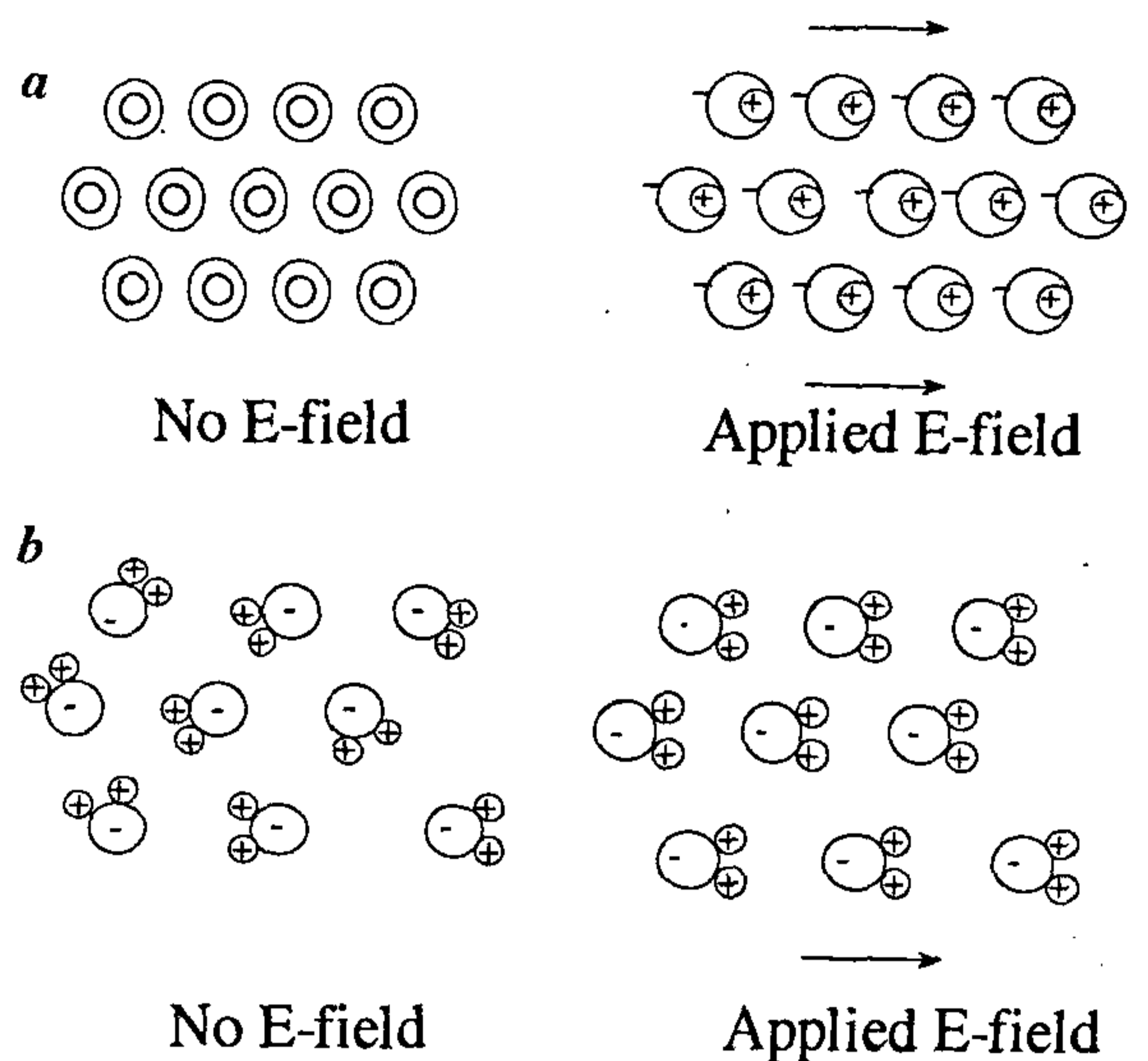


Figure 1. Electric polarization effects in simple models of a, non-polar material, and b, polar substance, e.g. H₂O.

which includes the excess bound charge, ρ_p , generated through the polarization process. Similarly Ampere's law, eq. (4), should include a polarization current term, J_p (see eq. (6)),

$$\nabla \times \frac{B}{\mu_0} = J + \frac{\partial \epsilon_0 E}{\partial t} + J_p. \quad (6)$$

All the above interaction mechanisms and the associated changes in Maxwell's equations can, however, be described by a property of the material known as the complex permittivity, ϵ^* .

$$\epsilon^* = \epsilon_0 \epsilon_r, \quad (7)$$

where ϵ_r is the relative permittivity, defined as the ratio of the electric displacement in a medium to that which would be produced in free space by the same field. The relative permittivity can be expressed in terms of real (ϵ') and imaginary (ϵ'') components.

$$\epsilon^* = \epsilon_0 (\epsilon' - j\epsilon''). \quad (8)$$

Here $j = \sqrt{-1}$. The real component, ϵ' , accounts for the additional polarization of bound charges, while ϵ'' represents the conduction of free charges, and is related to the conductivity σ by

$$\sigma = \omega \epsilon_0 \epsilon'', \quad (9)$$

where ω is the angular frequency of the time varying field.

Heat is produced by the interaction between the EM radiation and any conductive dielectric medium such as the tissue. The absorbed power density, W , resulting from both ionic conduction and vibration of dipole molecules, is given by

$$W = \frac{1}{2} \sigma |E|^2. \quad (10)$$

where $|E|$ is the magnitude of the electric field in the tissue. It is now important to emphasize the following points: (i) The propagation phenomenon is dominated by the conduction current at lower frequencies and by displacement currents resulting from the displacement of the dipoles in a dielectric at higher frequencies. Typical frequencies at which one phenomenon dominates over the other are strictly dependent on the dielectric medium. (ii) The mechanism by which power is absorbed in low frequency heating is fundamentally different from that which occurs during high frequency heating. In the former, the dimensions of the circuit elements are small compared to the wavelength of the RF and hence no attenuation is involved. At higher frequencies, the dimensions of the applicator are comparable to the wavelength and hence the propagating waves attenuate as they penetrate the lossy dielectric. While the upper limit of the frequency to be used is based on the required depth of penetration of the wave inside the body, the lower limit is determined by the electrical properties of the tissue cells.

Electrical properties of tissue cells

Tissues are composed of cells encapsulated by thin membranes containing the intracellular fluid composed of various salt ions, polar protein molecules and polar water molecules. The extracellular fluid has similar concentrations of ions and polar molecules, though some of the elements are different. As shown in Figure 2 *a*, when an electric current I approaches a biological cell, it will divide into two parts, one part will bypass the cell by means of its surrounding fluid, as characterized by the elements R_0 and C_0 in the circuit, while the other part will penetrate through the cell membrane, characterized in the circuit by the capacitors C_1 and the cell interior resistance R_1 . Figure 2 *b* shows a simplified equivalent electrical circuit corresponding to the electrical behaviour of tissues with high water content⁴. The cell membrane has a high capacitance per unit area of about $1 \mu\text{F}/\text{cm}^2$ and a resistance per unit area of more than $100 \Omega/\text{cm}^2$.

The reactance ($= 1/\omega C_1$; ω is the angular frequency of the EM wave) of the capacitors changes with frequency, thereby causing a frequency dependence of the ratio of the two currents entering and bypassing the cell. At

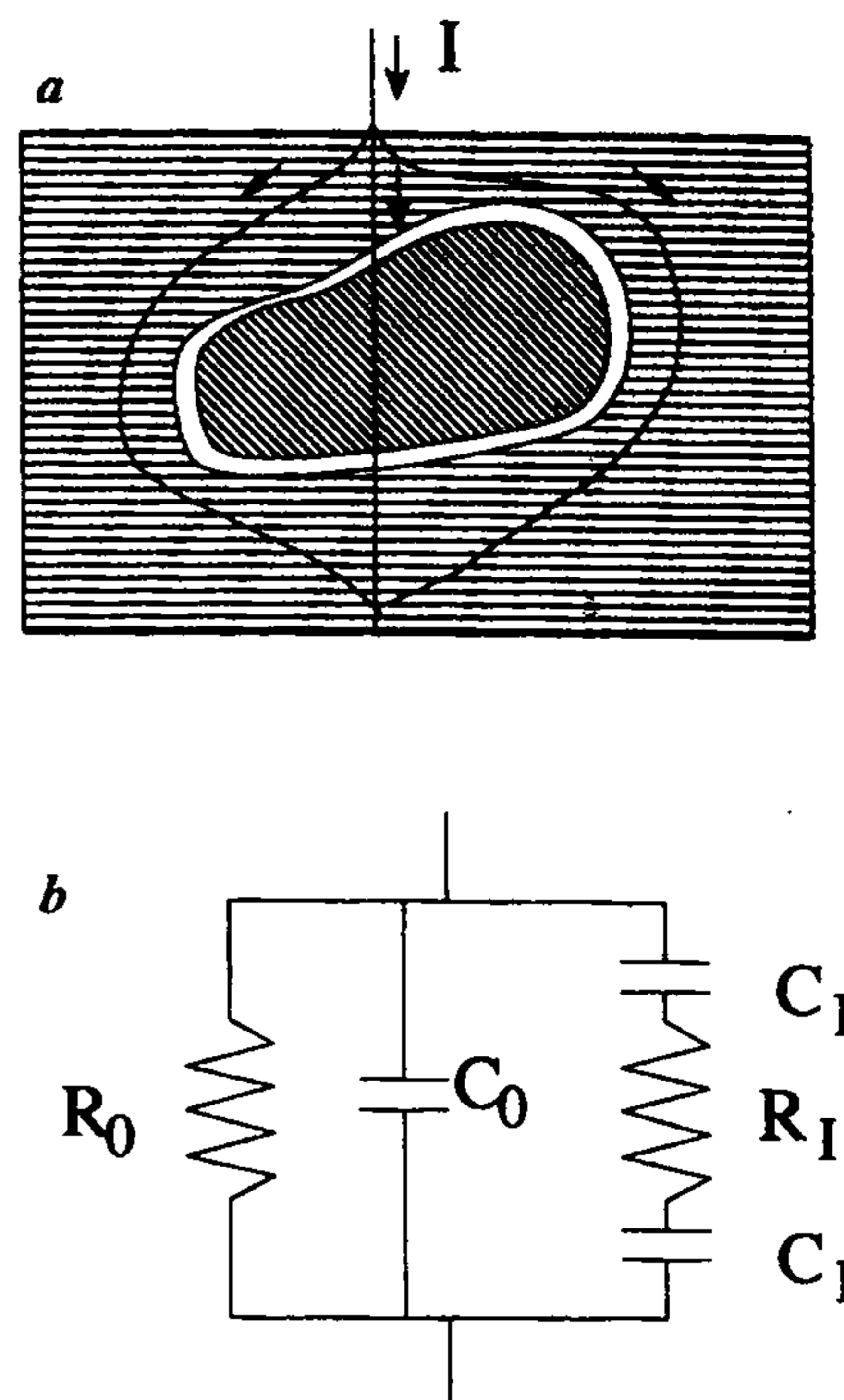


Figure 2. *a*, Diagrammatic representation of a cell; *b*, Equivalent circuit representing the electrical properties of biological cells. R_0 and C_0 are the resistance and capacitance of the fluid surrounding the cell, while C_1 and R_1 are the cell membrane capacitance and resistance of the fluid inside the cell, respectively (ref. 4).

frequencies over 100 Hz, the capacitive reactance of the cell membrane is so small that it may be assumed to be shorted out. Therefore, as long as one uses EM frequencies > 1 kHz, one will be able to short circuit the high reactance of the membrane and hence be able to heat the cytoplasm inside the cell. The capacitance of the cell membrane acts as an insulating layer at low frequencies so that current flows only in the extracellular medium, accounting for the low conductivity of the tissue.

σ increases with frequency, whereas ϵ' decreases with frequency. As the frequency increases, the capacitive reactance of the membranes decreases, resulting in an increase in the conductivity of the tissue. This can also be inferred from eq. (9). The decrease in ϵ' can be understood by considering the frequency of the EM field in relation to the time required to charge the cell membrane. As the frequency increases, insufficient time is available during each cycle to allow complete charging of the cell membranes. As a result, the total charge per cycle and the membrane capacitance decreases with increase in frequency. This is manifested as a decrease in ϵ' . Due to the low electrolyte content of fat, bone and other 'dry' tissues, the values of ϵ' and σ for these ma-

materials are an order of magnitude lower than those for tissues of high water content. These differences in σ and ϵ' are responsible for differential power absorption in various tissues.

RF hyperthermia

The term 'RF hyperthermia' covers a variety of techniques in which the elevation of temperature is achieved using EM power in the frequency range 1–100 MHz. The wavelengths associated with RF are considerably longer than the dimensions of parts of the human body. For example, at 13.56 MHz, a commonly used frequency, the wavelength in free space is 22 m. With a dielectric constant in the tissue as high as 100, this would still correspond to a wavelength in the tissue in excess of 2 m. Hence, RF can be used for heating deep-seated tumours. Due to the long wavelengths associated with RF, its electric and magnetic fields close to the applicator can be considered to be stationary. If the quasi-static B field is the major contributor to the heating process, then heating may be considered in terms of the induced electric field and the associated induced currents. If, however, the E field is dominant, then the heating process is discussed in terms of displacement or capacitive currents. However, conduction current is the major source of heating at such frequencies. A number of articles discuss the mechanisms of RF heating, its advantages and pitfalls⁵. The techniques used are referred to as capacitive and inductive heating; the main difference between these being in their differential absorption of power by different tissues. In this paper, inductive heating is discussed.

There are two common configurations of inductive-type applicators: a planar coil whose plane is parallel to the body surface, and a concentric coil surrounding the body (Figure 3). Here, the inductor is shown encircling the three concentric layers of non-magnetic lossy dielectric, representing respectively, skin, subcutaneous fat, and muscle. The RF current is terminated in the applicator which emits a rapidly varying magnetic field. Since biological materials are essentially non-magnetic, the time-varying magnetic field passes through the tissues unperturbed, inducing eddy currents in the conductive tissues. Maxwell's equations, which must be satisfied in the region encompassed by the inductor, require that the flux lines of the E field be concentric circles if the magnetic field is axially directed inside the coil. Hence, the E field at a boundary between layers is tangential to the boundary and has the same value on each side of the boundary. Thus, for example, $E_m = E_n$, with E_m and E_n representing the E field at the m th and n th layer. The heat generated at these two points, in W/m^3 , is in the ratio

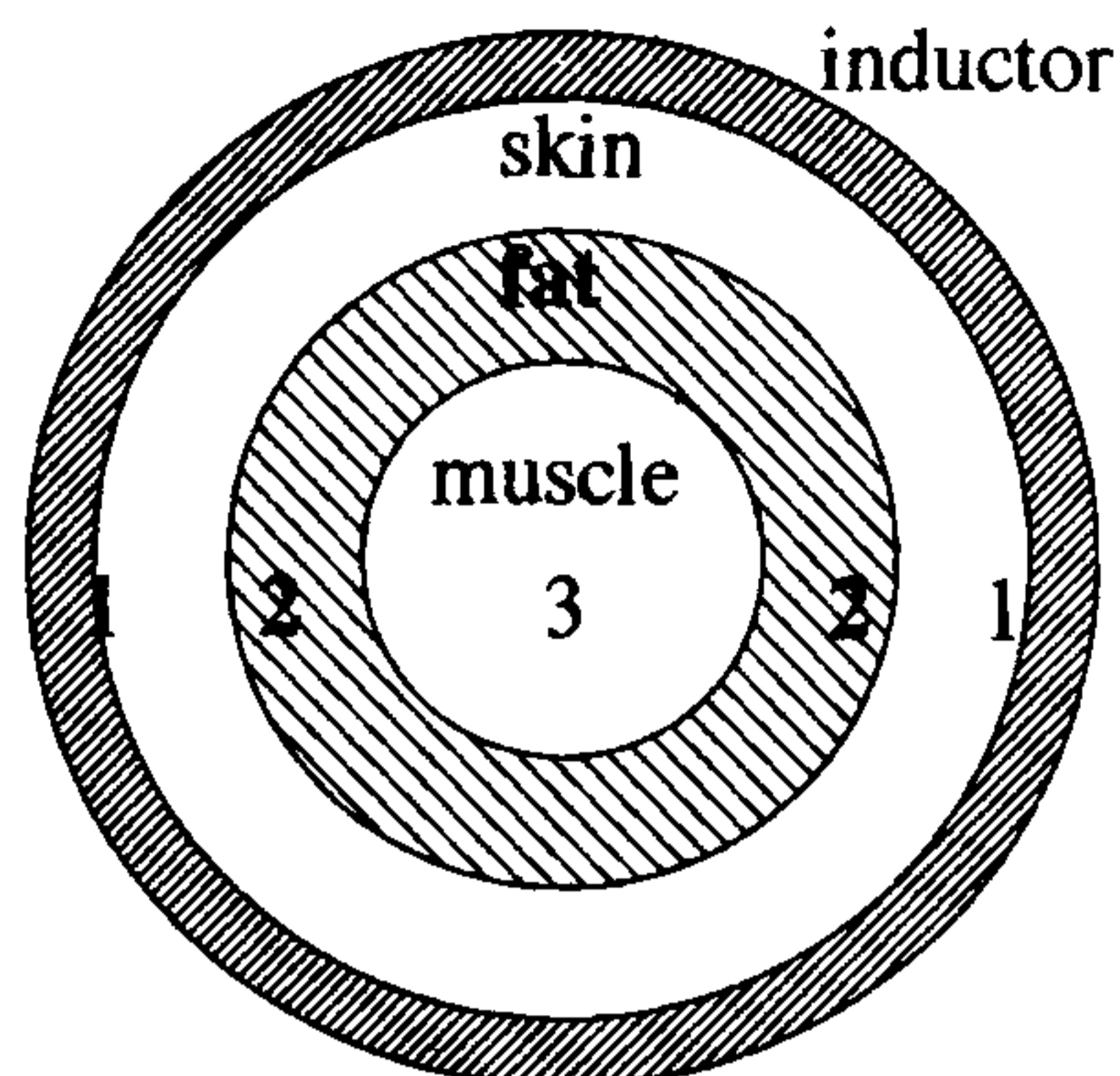


Figure 3. Model of an inductor-type hyperthermia electrode.

$$\frac{H_m}{H_n} = \frac{\sigma_m |E_m|^2}{\sigma_n |E_n|^2} = \frac{\sigma_m}{\sigma_n} \quad (11)$$

With this method of heating, the heat generated in the subcutaneous fat layer is only 20–70% of that generated in the skin or muscle layers⁴. Thus, if the electric field is oriented parallel to the layer interfaces, excessive unwanted heating of the fat layer (which has higher resistivity than most other tissues) can be significantly reduced. Frequencies in the range 10–35 MHz are commonly employed for inductive heating.

In principle, all the coils (both capacitive and inductive) mentioned above can be used in an MR set-up enabling simultaneous delivery of hyperthermia (within the magnet) and MR studies. The choice of the heating method, however, is usually based on the accessibility of the experimental tumour, the heating techniques available and the type of experiment planned. Since the aim of the work presented here was to apply hyperthermia within the magnet along with the experimental set-up for MR studies, RF hyperthermia was chosen so that the RF source used in MR experiments for exciting the nuclei can be used for delivering hyperthermia. There remains then the choice between capacitive and inductive heating. For this study, the RF coil was designed such that the transmitter/receiver coil (a single loop surface coil) for the MR experiments was used as an inductive hyperthermia device⁶.

Methods

This study presents work in which ³¹P MRS and a fibre-optic pH meter [Cardiomet 4000TM (Biomedical Sensors Ltd, Kansas City, USA)] were used simultaneously to follow the changes in tumour bioenergetics and extracellular pH (pH_e), respectively, of murine RIF-1 tumours

during and after RF hyperthermia. The same coil (a single loop 1.2 cm diameter surface coil) was used both for the MR study and for delivering hyperthermia at 34 MHz, the phosphorus frequency at 2.0 T. The development of the hyperthermia system used in this study and the extensive preliminary experiments (both on phantoms and mice) have been fully discussed elsewhere⁶⁻⁹.

The tumour was grown subcutaneously in the lower dorsal area of female C3H/km mice, just above the tail. All the experiments were carried out on unanesthetised mice. The coil was placed 2 mm from the shaven surface of the tumour, and heating was carried out at 15 watts; reflected power was kept within 2-3% of the forward power. Tumour temperature was recorded at the centre using specially constructed constantan-manganin thermocouples of outer diameter 320 μm (ref. 9). Rectal temperatures were monitored with similar thermocouples, but of outer diameter 480 μm . Temperatures were read every 4 min using a digital thermometer (12 way Type T selector unit, Model 2751-T, Digitron Instrumentation Ltd) which was located well away from the magnet, requiring the construction of special thermocouples with long leads.

Heat delivery was controlled by an electronic feedback mechanism which monitored the temperature difference between the target and measured (central) tumour temperature and adjusted the duration of the 'power on' phase within the 10 s heating cycle time. All temperature measurements were made during the power-off period. The temperature selected for investigation of the effects of hyperthermia on tumour bioenergetics and pH_e was 44°C delivered for 30 min. pH_e was monitored every 4 min before, during and after heating.

In vivo ^{31}P MRS was carried out at the phosphorus frequency of 34 MHz, using an Oxford Research Systems Biospec II console, with an Oxford Instruments 31 cm horizontal bore 2.0 T superconducting magnet. Adiabatic pulses were used for uniform excitation of the sample¹⁰. ^{31}P spectra (starting at 30 min after immobilization) were acquired approximately every 30 min over a period of about 2.5 h. A delay interval of two seconds and 1000 scans were used. Spectra were processed using the deconvolution-difference method by using 25 Hz and 1000 Hz line-broadening.

Results

Figure 4 shows a typical tumour heating profile observed during 30 min at 34 MHz. Profiles for both the centre and surface of the tumour are presented; also shown is the simultaneously recorded pH_e in the centre of the tumour. The uniformity of heating is evident from the similarity of temperatures recorded at the tumour centre and periphery. Figure 5a shows a typical ^{31}P MR

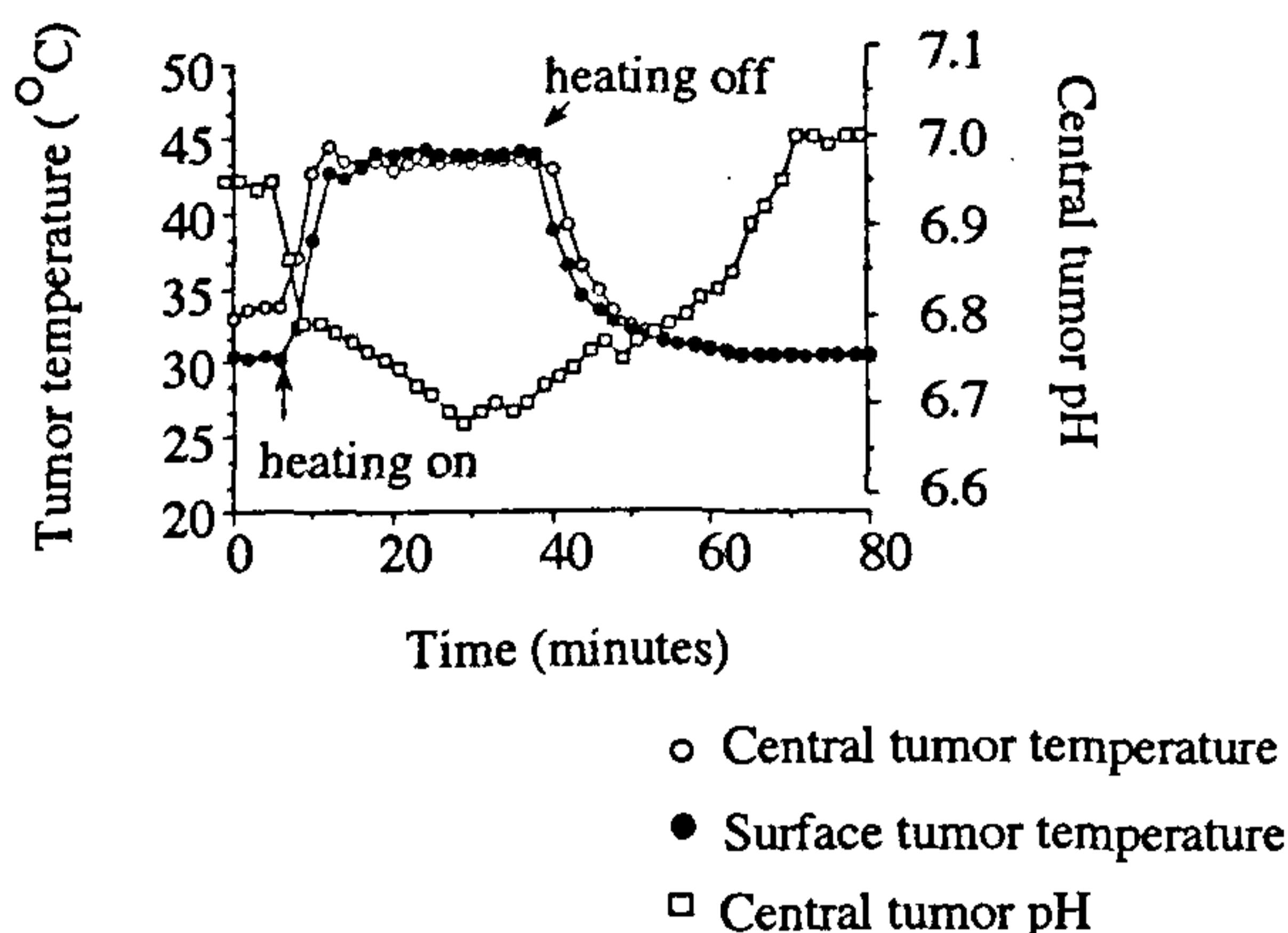


Figure 4. Effect of heating a RIF-1 tumour at 34 MHz at a power level of 15 watts for 30 min on surface and central tumour temperatures and central extracellular pH.

spectrum obtained *in vivo* from untreated RIF-1 tumours. The assignment of resonances to phosphomonoester (PME), Pi, phosphodiester (PDE), PCr, γ -nucleotidetriphosphate (γ -NTP), α -NTP, and β -NTP were made from published results¹¹. The spectrum shows a high level of PME and high energy phosphates. Representative spectrum 2.5 h after hyperthermia is shown in Figure 5b. It can be seen that there is no recovery of NTP and other phosphate metabolites at this time point, i.e. 2.5 h after hyperthermia, except for the presence of a large Pi peak relative to the PME peak, indicating cell damage in this tumour. A similar pattern was observed at the different time points studied. Intracellular pH was also determined but is not discussed here.

Discussion

The aim of the present study was testing the feasibility of delivering hyperthermia within the magnet using the MR RF coil and the simultaneous study of some tumour physiological parameters of importance to hyperthermia. Hence, physiological changes resulting from hyperthermia are discussed only sparingly. The increased level of Pi seen after 44°C treatment is taken to indicate damaged cells. Although it was initially thought that a breakdown of PCr and NTP to Pi was an integral part of the necrotic process following cell death, it is now known that there is no direct relationship between Pi and necrotic fractions¹². The high Pi signal would therefore not arise from necrosis following cell death but from damaged cells in a prelethal state.

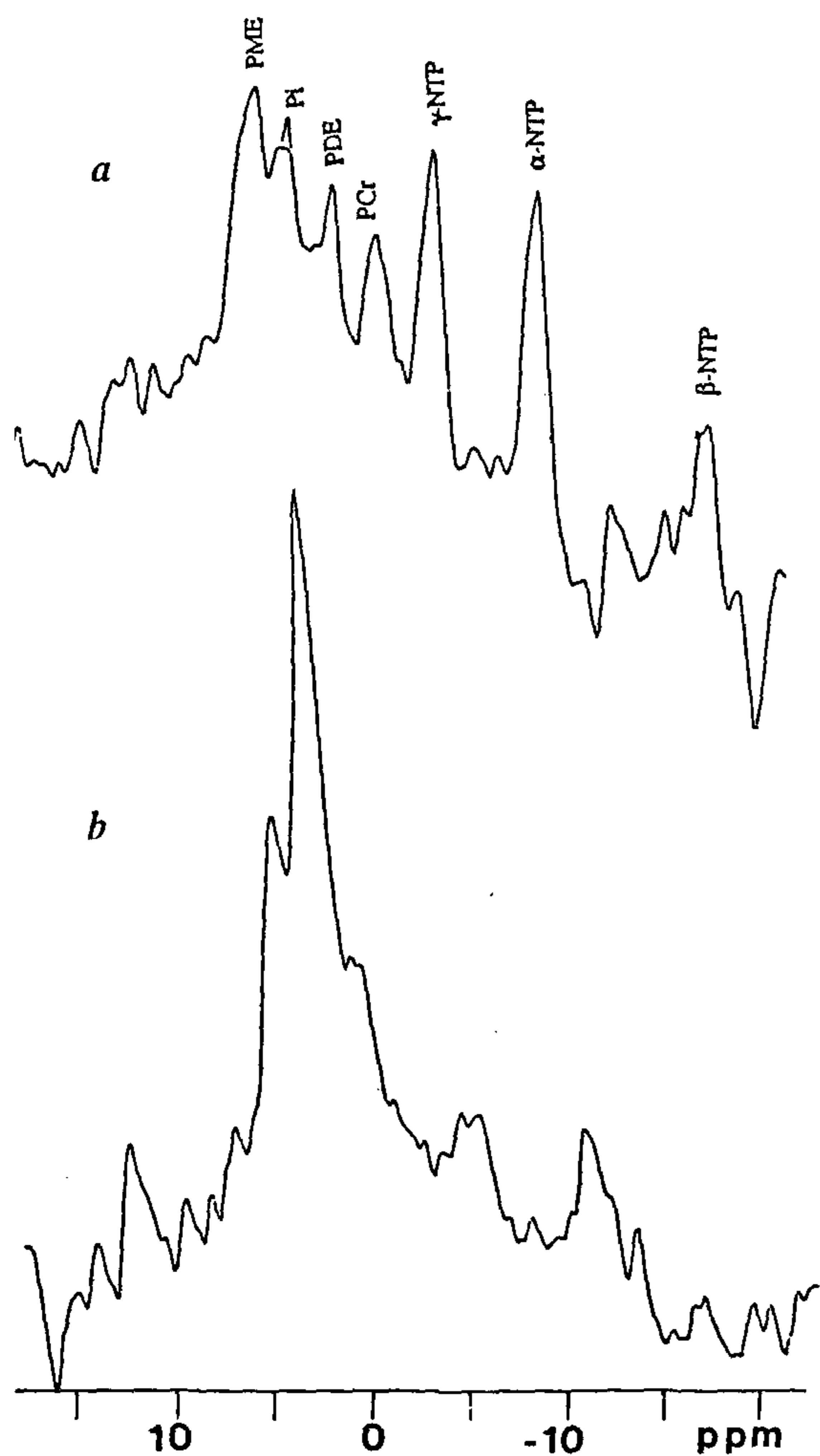


Figure 5. ^{31}P spectra from a RIF-1 tumour. *a*, Spectrum obtained before hyperthermia; *b*, spectrum obtained 2.5 h after 30 min of hyperthermia at 44°C .

Hyperthermia as a cancer treatment modality is still in the experimental stage. Although hyperthermic cell killing has been demonstrated in many *in vitro* studies, the mechanisms underlying cell damage and death have not been fully elucidated. Further work is required towards this end, and information from non-invasive studies on the effects of hyperthermia on tumours *in vivo* will be extremely valuable. In this study a successful combination of hyperthermia delivery and non-invasive study of tumour pH and tumour bioenergetics using MR has been achieved. Further studies along these lines and also on other aspects of tumour metabolism are required in order to develop the rationale for and optimization of hyperthermia as a cancer therapy. It is believed that data arising from such experiments, as presented in this study, will bring about greater understanding of what hyperthermia might accomplish clinically. The authors hope that this will also open up a variety of work combining MR and hyperthermia.

1. Storm, F. K. (ed.), *Hyperthermia in Cancer Therapy*, G. K. Hall Medical Publishers, Boston, 1983.
2. Curran, W. J. and Goodman, R. L., in *Radiation Research: A Twentieth-Century Perspective* (eds Dewey, D. C., Edington, M., Fry, R. J., Hall, E. J. and Whitmore, G. F.), Academic Press, San Diego, 1992, pp. 883–888.
3. Stratton, J. A. (ed.), *Electromagnetic Theory*, McGraw-Hill, 1941.
4. Schwan, H. P. and Piersol, G. M., *Am. J. Phys. Med.*, 1954, **33**, 371–404.
5. Wust, P., Stahl, H., Loeffel, J., Seebars, M., Riess, M. and Felix, R., *Int. J. Hyp.*, 1995, **11**, 151–167.
6. Jayasundar, R., Ph D Dissertation, University of Cambridge, 1990.
7. Jayasundar, R., Hall, L. D. and Bleehen, N. M., *NMR Biomed.*, 1992, **5**, 360–363.
8. Jayasundar, R., Hall, L. D. and Bleehen, N. M., *Magn. Reson. Imaging*, 1997, **15**, 847–855.
9. Jayasundar, R., Hall, L. D. and Bleehen, N. M., *Australas. Radiol.*, in press.
10. Bendall, M. R. and Pegg, D. T., *J. Magn. Reson.*, 1986, **647**, 376–381.
11. Evanochko, W. T., Sakai, T. T., Ng, T. C., *et al.*, *Biochim. Biophys. Acta*, 1984, **805**, 104–116.
12. Tozer, G. M. and Griffiths, J. R., *NMR Biomed.*, 1992, **5**, 279–289.